

---

# CatLC: Catalonia Multiresolution Land Cover Dataset

---

**Carlos García Rodríguez**  
Institut Cartogràfic i  
Geològic de Catalunya &  
Universitat de Barcelona  
c.garcia.r@icgc.cat

**Oscar Mora**  
Institut Cartogràfic i  
Geològic de Catalunya  
oscar.mora@icgc.cat

**Fernando Pérez-Aragüés**  
Institut Cartogràfic i  
Geològic de Catalunya  
fernando.perez@icgc.cat

**Jordi Vitrià**  
Universitat de  
Barcelona  
jordi.vitria@ub.edu

## Abstract

1 Traditional natural image datasets are very rich. However, only a few remote  
2 sensing datasets are available and cover a tiny territory or cover a larger one with  
3 low spatial resolution and/or few classes. In this paper, we present the *Catalonia*  
4 *Multiresolution Land Cover Dataset* (CatLC), a remote sensing dataset. The  
5 dataset contains images at different spatial resolutions captured by both aircraft  
6 and satellites (Sentinel-1 and Sentinel-2), in addition to topographic maps. All  
7 this dataset has been created with images from the Cartographic and Geological  
8 Institute of Catalonia (ICGC) catalogs and the European Space Agency (ESA).  
9 The ICGC's land cover ground truth accompanies these images with 41 classes at a  
10 spatial resolution of 1 m in an area of 32000 km<sup>2</sup>, covering the Spanish region  
11 of Catalonia. CatLC is a multilayer, multiresolution, multimodal, multitemporal  
12 dataset, which has excellent potential for the Artificial Intelligence (AI) community  
13 and the exploration of modeling methodologies. Land cover maps are used in  
14 different realms such as forestry for inventory area estimates, hydrology regarding  
15 microclimatic variables, agriculture to improve irrigation or geology in geohazards,  
16 and risk identification and assessment. Therefore, accurate and updated knowledge  
17 about land changes is essential for territory management with different purposes  
18 over multiple fields. Using various combinations of the images from the dataset,  
19 we offer a benchmark that could serve as a starting point to explore artificial  
20 intelligence techniques for remote sensing segmentation purposes. In this vein,  
21 CatLC dataset aims to engage with computer vision experts interested in remote  
22 sensing and stimulate research and development. [The CaTLC dataset is avail-  
23 able at https://www.icgc.cat/en/Downloads/Aerial-and-satellite-  
24 images/Contingut/Catalonia-Multi-resolution-Landcover-Dataset-  
25 CatLC.](https://www.icgc.cat/en/Downloads/Aerial-and-satellite-images/Contingut/Catalonia-Multi-resolution-Landcover-Dataset-CatLC)

## 26 1 Introduction

27 [Pixel-wise, human annotation of satellite images is challenging and dubious and thus often requires  
28 manual annotation with tools like Google Street View, fieldwork, etc. Therefore, mapping agencies  
29 are on the quest to explore](#) how to substitute their strenuous and time-consuming manual tasks for  
30 automated processes. To do so, current accuracy in automatic land cover segmentation requires  
31 improvement in terms of methodologies and data coming from airborne and satellite sensors. Land



Figure 1: Continuous area using different layers of the dataset together with the ground truth.

32 cover segmentation is among the primary uses of airborne and satellite images and the proposed  
 33 focus of this work.

34 Land cover maps are used in different realms such as forest inventory or forest management, hydrology  
 35 regarding microclimatic variables, agriculture to improve crop management or geology in risk  
 36 identification and assessment. Therefore, accurate and updated knowledge about land dynamics is  
 37 essential for territory management with different purposes and in multiple fields. These land cover  
 38 maps are provided by institutions that invest time and human resources to fulfill the costly task of  
 39 producing them.

40 In cartographic institutions, due to their heritage, legal assessments and administrative framework,  
 41 land segmentation is still done mainly employing photointerpretation techniques, entailing very high  
 42 costs in terms of time and human resources. Thus, cartographic institutes are transitioning from  
 43 manual land segmentation to automation [1]. The transformation towards an automatic solution tends  
 44 to face a critical point: the scarcity of high-quality datasets. In this regard, we find datasets composed  
 45 of canonical images such as ImageNet[2] and PASCAL VOC Dataset [3]. Labeling the images of  
 46 such datasets does not pose an interpretation problem as they are distinctive. However, labeling aerial  
 47 images correctly might be challenging, i.e., to differentiate between the deciduous or evergreen forest.

48 In this paper, we present the Catalonia Multiresolution Land Cover Dataset (CatLC). This dataset  
 49 comprises a large variety of images: orthophoto RGB and infrared from airborne sensors at high  
 50 resolution, radar from satellite sentinel-1, multispectral from satellite sentinel-2, and composition  
 51 of topographic maps—all those accompanied by a land cover map minutely labeled by experts  
 52 in photointerpretation. Using different combinations of the images from the dataset, we offer a  
 53 benchmark that could serve as a starting point to explore different artificial intelligence techniques  
 54 for remote sensing segmentation purposes. CatLC dataset aims to engaging with computer vision  
 55 experts interested in remote sensing and stimulate research and development.

## 56 2 Previous work

57 In 2017, a competition was held to find the best automatic labeling algorithm for two German cities,  
 58 preparing two different datasets [4]. The first one was in Vaihingen, and the dataset was composed of  
 59 38 different tiles and consisted of an orthophoto (infrared, red, and green bands) and a Digital Surface  
 60 Model (DSM). The resolution (ground sampling distance) of the orthophoto and the DSM was 9 cm.  
 61 The second one in Potsdam consisted of an orthophoto (4 bands including infrared) and a DSM, all at  
 62 5 cm spatial resolution. These data were arranged in 38 tiles. Ground truth consisted of six classes:  
 63 impervious surfaces, buildings, low vegetation, trees, cars, and background. Both datasets had a very  
 64 high resolution, but they covered a small area.

65 There is also the Inria (France) dataset that covers an area of 810 km<sup>2</sup> comprising an orthophoto layer  
 66 at a spatial resolution of 30 cm and ground truth consisting of two classes (building/no-building) in  
 67 several cities with different populations, from downtown San Francisco to alpine cities in Austria [5].  
 68 Another example of the use of remote sensing is the SpaceNet Road Network Detection dataset. This  
 69 dataset has more than 8000 km of roads and four cities: Las Vegas, Paris, Shanghai, and Khartoum.  
 70 The purpose of this dataset is to find the roads and classify them into 7 different types [6].

71 In addition, a few years ago, the US Geological Survey released a land cover dataset of the state of  
 72 New York where we can find 21 classes at a spatial resolution of 30 m per pixel [7]. Finally,  
 73 DLR (German Aerospace Center) also produced a dataset comprising 31 semantic categories and  
 74 12 subcategories of lane markings for different German and European cities. This dataset contains

Table 1: Summary of some of the most used datasets in remote sensing applications for land cover segmentation compared to CatLC. Some datasets do not specify the resolution at which the ground truth was labeled.

Dataset	Bands	Classes	Tiles	Tile shape (pixels)	Ground truth resolution (m/pixel)
Vaihingen	5	6	38	2000 × 2000	unknown
Potsdam	5	6	38	6000 × 6000	unknown
Inria	3	2	180	5000 × 5000	0.3
USGS New York	-	21	1	16989 × 22610	30
SkyScapes (DLR)	3	31	16	5616 × 3744	13
FloodNet	3	10	~ 400	4000 × 3000	unknown
CatLC	21	41	34040	960 × 960	1

75 16 images of size 5616 × 3744 at 13 cm spatial resolution [8]. More recently, we find the Floodnet  
 76 dataset, which provides high-resolution UAS imageries with detailed semantic annotation [9]. In  
 77 Table 1 we summarize the description of the aforementioned individual datasets.

### 78 3 CatLC: Catalonia Land Cover Dataset

79 In this section, the CatLC dataset is presented in detail, consisting of a set of images obtained by airborne and  
 80 satellite sensors from the catalogs of the Cartographic and Geological Institute of Catalonia (ICGC) and the European  
 81 Space Agency (ESA), and the current ICGC’s land cover map.  
 82  
 83  
 84

85 It covers the entire territory of Catalonia (Spain), approximately 32000 km<sup>2</sup>, providing an extraordinary source of  
 86 information for the application of AI and Deep Learning (DL) techniques, both regarding the quality and variety  
 87 of the images and their extension, not limited to a small part of the territory. Catalonia is located on the shores  
 88 of the Mediterranean Sea and has a great variety of types of land cover, which makes it very suitable to create a  
 89 heterogeneous dataset with numerous labels.  
 90  
 91  
 92  
 93



Figure 2: Location of the area of interest, Catalonia (Spain).

94 All the images have been acquired during 2018 at different spectral bands and spatial resolutions and are provided in GeoTiff raster format. They all share a  
 95 common georeferencing at WGS84 UTM31N Reference System projection and they cover the same geographic extension, given by the following bounding box: UTM X West: 240000, UTM X East:  
 96 540000, UTM Y North: 4780000, and UTM Y South: 4480000. The different types of images, with spatial resolutions that vary between 1 and 10 meters, depending on the product and sensor used,  
 97 are presented in detail in the following subsections. In such subsections we also illustrate the bands provided by the dataset (land cover, orthophoto, Sentinel-1, Sentinel-2 and topographic maps). The  
 98 figures 4, 5, 6, 7, 8, 9, 10,11, 12, show the different bands on three geographical areas in Catalonia (area A: 42°08’02.6”N 1°29’30.7”E, area B: 42°02’23.0”N 2°39’56.0”E and area C: 41°57’50.3”N  
 99 2°08’42.4”E). We have summarized all available data in Table 3.  
 100  
 101  
 102  
 103  
 104

#### 105 3.1 Land Cover Map

106 The 2009 land cover map presented here is a simplification to 41 classes of the Land Cover Map of Catalonia (version 4) generated by CREAM (Center for Ecological Research and Forestry Applications) [10], together with an adaptation to the data model approved by the Cartographic Coordination  
 107 Commission of Catalonia which allows the comparison between maps of different years.  
 108  
 109

110 The 2018 land cover map is an update of the 2009 map, made from the photointerpretation of ICGC’s 2018 orthophotos. The minimum area for labeling an element was 500 squared meters and the  
 111

Table 2: CatLC Dataset with 41 classes and legend.

<b>Agricultural area</b>		14 Meadows and grasslands	28 Sports and leisure areas	
01 Herbaceous crops		15 Shore forest	29 Mining or landfills	
02 Orchard, plant nurseries...		16 Bare forest soil	30 Areas in transformation	
03 Vineyards		17 Burned areas	31 Road network	
04 Olive groves		18 Rocky	32 Urban bare ground	
05 Other woody crops		19 Beaches	33 Airport areas	
06 Crops in transformation		20 Wetlands	34 Railway network	
<b>Forest area</b>		<b>Urban area</b>		
07 Dense coniferous forests		21 Urban area	<b>Water bodies</b>	
08 Dense deciduous forests		22 "Eixample"	36 Reservoir	
09 Dense forests of sclerophylls		23 Lax Urban Areas	37 Lakes and lagoons	
10 Scrub		24 Isolated buildings	38 Watercourses	
11 Clear coniferous forests		25 Isolated residential areas	39 Rafts	
12 Clear deciduous forests		26 Green areas	40 Artificial channels	
13 Clear forests of sclerophylls		27 Industrial or commercial	41 Sea	

112 minimum length for linear features such as roads, rivers, railroad tracks, etc. was between 8 and 10  
 113 meters. The working scale for the photo-interpreters has been 1:2500. The changes bigger than 2 ha  
 114 in extent have been identified using the following information:

- 115 • Comparison of LANDSAT images of both years, 2009 and 2018.
- 116 • The changes reflected in ICGC's 1: 5000 Topographic Base.
- 117 • The forest fires and the SIGPAC (Geographic Information System of Agricultural Plots)  
 118 data for this period.

119 The change layer between 2012 and 2018 of the Corine Land Cover has also been considered and  
 120 special attention has been paid to the categories of crops in transformation and zones in transformation  
 121 of the 2009 version due to their greater dynamics.

122 Exceptionally, due to the large volume of changes in the agricultural areas of Lleida and the coastal  
 123 area from Tarragona to Barcelona, only agricultural changes of more than 5 hectares have been photo-  
 124 interpreted. Supervision has been performed on a sample of 811 points throughout this territory,  
 125 resulting in a thematic accuracy of 81%. The final 41-class (see Table 2) product presented in this  
 126 publication is delivered at spatial resolution of 1m. [The distribution of the land covers along the](#)  
 127 [territory is heterogeneous. Some covers as herbaceous crops or dense coniferous forests are way more](#)  
 128 [common than airport areas or rafts. In Figure 3, we can see the histogram for the complete dataset.](#)

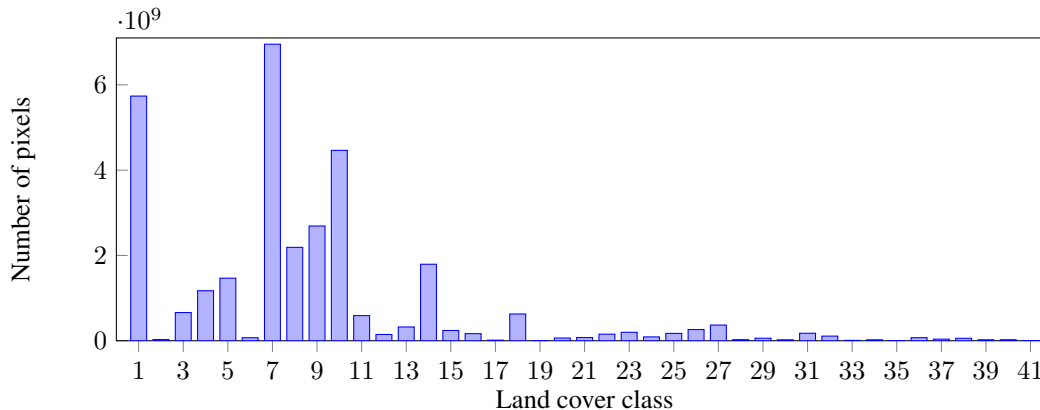


Figure 3: Class distribution on CatLC dataset.

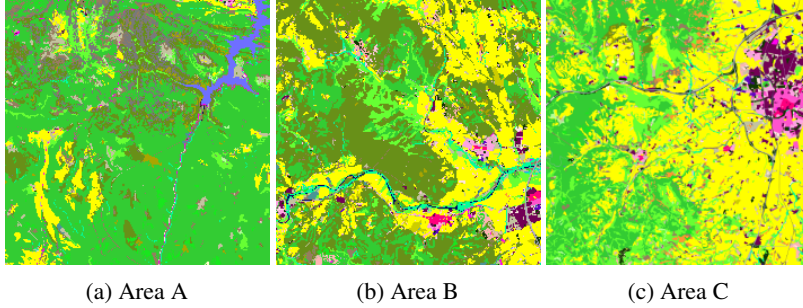


Figure 4: Land cover map samples.

129 **3.2 Orthophoto**

130 An orthophoto is a cartographic document consisting of a vertical aerial image that has been rectified  
 131 in such a way as to maintain a uniform scale over the entire image surface. It consists of a geometric  
 132 representation at a given scale of the Earth's surface. The original images were taken with a res-  
 133 olution of 25 centimeters ([https://www.icgc.cat/en/Downloads/Aerial-and-satellite-  
 134 images/Conventional-orthophoto](https://www.icgc.cat/en/Downloads/Aerial-and-satellite-images/Conventional-orthophoto)), but because the land cover map has a resolution of 1 meter,  
 135 we have decided to rescale the orthophoto raster layer also to 1 meter.

136 This layer comprises four distinct bands, each providing information from different zones of the  
 137 electromagnetic spectrum. Three of them belong to the visible area of the spectrum (RGB) and one  
 138 of them to the infrared area. On this cartographic document, digital make-up tasks have been carried  
 139 out to minimize artifacts that may have originated during the generation process or the acquisition of  
 140 the images. This way, it can be assured that the affected area does not exceed 1% of the total area of  
 141 Catalonia.

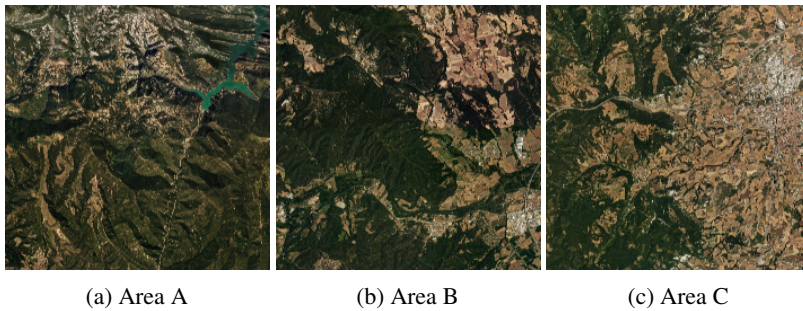


Figure 5: Orthophoto RGB samples.

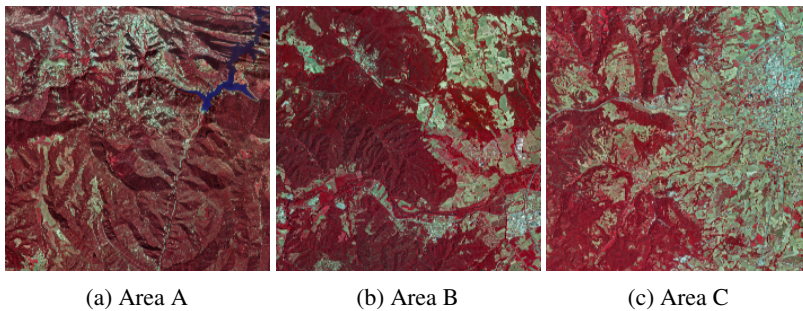


Figure 6: Orthophoto (Infrared,R,G) samples.

142 **3.3 Sentinel-1**

143 The Sentinel-1 dataset has been generated from radar images (Synthetic Aperture Radar, SAR) in  
144 GRD (Ground Range Detected) mode from the year 2018 at 10-meter spatial resolution. The Sentinel-  
145 1 satellite constellation is made up of two twin satellites, A and B, from the European Space Agency  
146 (ESA). These satellites emit a microwave signal (frequency 5.405 GHz) and subsequently receive the  
147 echo of the reflection on the ground surface. Therefore, Sentinel-1 images contain information on  
148 the reflectivity of the terrain, which depending on its type (urban, vegetation, crops, water, etc.) will  
149 have a different intensity, thus providing valuable information for its classification. For this purpose,  
150 12 acquisitions have been chosen, one for each month of the year, covering the entire territory of  
151 Catalonia. Full coverage has been achieved by combining 2 orbits in ascending mode (orbits 30 and  
152 132) and VV (Vertical-Vertical) polarizations in similar dates. **The descending orbit and VH (Vertical-  
153 Horizontal) polarization have not been included in the present dataset because the information is  
154 mostly redundant. However, its use can be explored in case it provides improvements in segmentation.**  
155 Additionally, an average image of the year 2018 has been generated with improved radiometry  
156 (multitemporal speckle reduction) by combining all 12 monthly images into one. Consequently, the  
157 average image cannot provide information on temporary changes during 2018 providing however a  
158 lower noise level. In appendix B we explain how the Sentinel-1 images are generated.

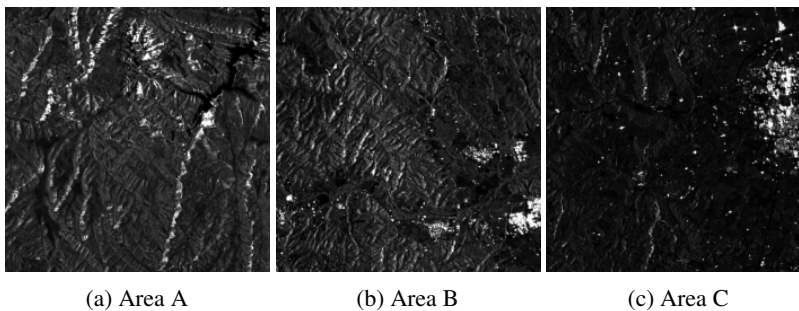


Figure 7: Sentinel-1 (average image during 2018) samples.

159 **3.4 Sentinel-2**

160 Sentinel-2 provides multispectral imagery data at different resolutions approximately every five days.  
161 We have selected two relevant dates for this dataset, the first one in April and the second one in  
162 August. We have chosen these two dates to follow the phenological evolution of the vegetation  
163 throughout the spring and late summer. As we are in the Mediterranean area, with these two dates it  
164 is possible to detect both winter and summer herbaceous crops as well as evergreen and deciduous  
165 forest masses. Due to the presence of clouds, multiple data takes have been necessary to make a  
166 cloud-free mosaic. In appendix B we explain how the Sentinel-2 images are generated.

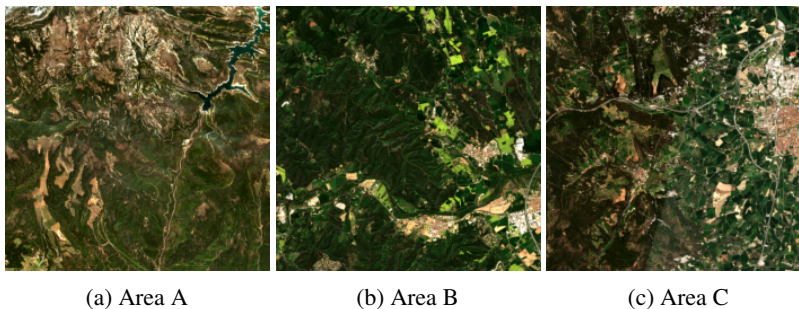


Figure 8: Sentinel-2 RGB (April 2018) samples.

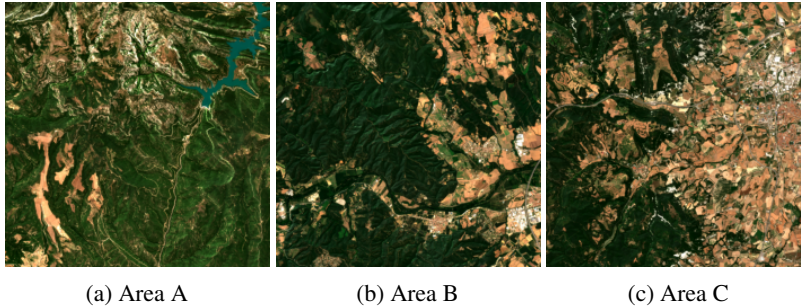


Figure 9: Sentinel-2 RGB (August 2018) samples.

167 **3.5 Topographic Maps**

168 Three different topographic products and two subproducts have been generated. Their characteristics  
 169 are outlined in the following paragraphs.

170 **3.5.1 Digital Elevation Model**

171 This is a standard layer freely distributed by ICGC and is built upon the altimetric information of  
 172 the Topographic Base of Catalonia 1:5000 version 2 (BT-5m v2.0) that includes profiles, altimetric  
 173 coordinates, breaklines and contour lines, all of them obtained from the terrain. It consists of a raster  
 174 image at 5m pixel size and its estimated altimetric accuracy is 0.9m RMS.

175 Two typical subproducts for remote sensing applications are the slope, which indicates each pixel's  
 176 steepness, and the aspect that indicates the orientation of the maximum slope between adjacent  
 177 pixels. These values have been calculated from the Digital Elevation Model. Therefore they contain  
 178 redundant information. We include them because they might be helpful for the interpretation of the  
 179 results.

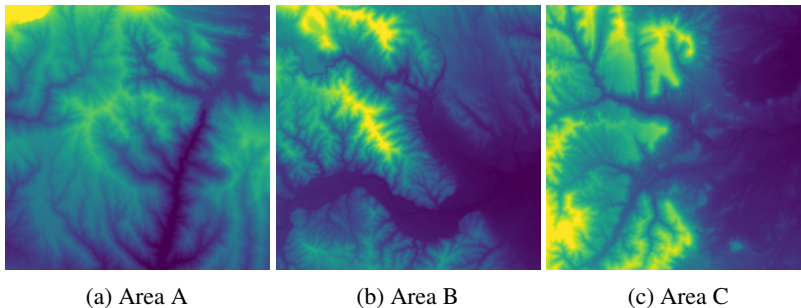


Figure 10: Digital Elevation Model (DEM) samples.

180 **3.5.2 Digital Surface Model**

181 This is a raster layer at 1m pixel size containing orthometric heights obtained by automatic correlation  
 182 between aerial photogrammetric images at 0.25m - 0.35m. It represents the topmost height for every  
 183 pixel position on the grid be it the ground or, mainly, forest canopy and buildings.

184 **3.5.3 Canopy Height Model**

185 The Canopy Height Model (CHM) is a high resolution (1m) raster dataset that maps all the objects  
 186 over the terrain as a continuous surface. It is advantageous to delineate the forest extent, but it also  
 187 includes urban landscape data. Each pixel of this model represents the height of the trees above the  
 188 ground topography. In urban areas, the CHM represents the height of buildings or other built objects.

189 This layer is built through subtraction of the 2016-2017 LIDAR Digital Elevation Model (<https://www.icgc.cat/en/Downloads/Elevations/Lidar-data>) from the 2018 photogrammetric  
 190

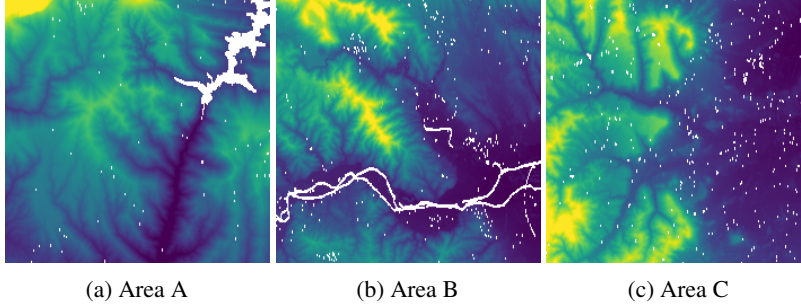


Figure 11: Digital Surface Model (DSM) samples.

191 Digital Surface Model. To clarify, this product is not dependent on the previous Digital Elevation  
 192 Model. This DEM is produced by LIDAR and the one in the dataset by aerial images.

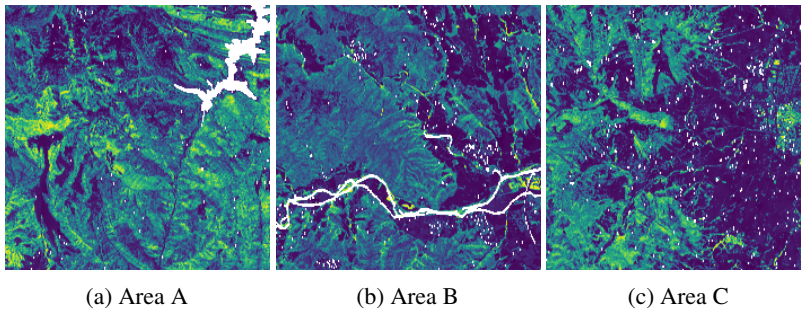


Figure 12: Canopy Height Model (CHM) samples.

Table 3: Summary of CatLC dataset.

Data	Independent bands	Resolution (m)
Orthophoto	4	1
Sentinel-1	12	10
Sentinel-2	20	10
Digital Elevation Model	1	5
Digital Surface Model	1	1
Canopy Height Model	1	1
Land Cover Map	-	1

34040 images at  $960 \times 960$  pixels per source of 1m data

## 193 4 Experiments

194 An initial benchmark accompanies the CatLC dataset to have a starting point and show a helpful  
 195 pipeline to train a model with raster images. Unlike other datasets that have multiple images, CatLC  
 196 has only one big image. To work with it, we will need to access smaller tiles, so the first step has been  
 197 to create a list with the indexes of all the tiles that we are going to use in the dataset of dimension  
 198  $960 \times 960$  pixels (in the higher spatial resolution images of 1 m). This list was then randomly  
 199 divided into three groups, 60% for training, 20% for validation, and 20% for testing. Being this is a  
 200 segmentation problem, we have not been able to have a homogeneous distribution of the three groups  
 201 because usually, tiles contain multiple classes. The distribution for the sets can be found in Annex C.

202 As a first use case, we have selected the classical U-Net neural network the [11], which is used as a  
 203 starting point in most applications that require image segmentation. The experiments are implemented  
 204 in PyTorch, running in a workstation with a Nvidia Quadro P5000 GPU. Cross entropy loss has been  
 205 used, together with a commonly used Adam optimizer with 0.0001 as the learning rate.

206 The experiments have considered three different scenarios:

- 207 1. Use as input data orthophoto RGB and infrared. We know by experience that the high  
208 resolution should give good results in the frontier of the classes, but its lack of more  
209 spectral bands makes it harder to differentiate classes that belong to the agricultural or forest  
210 superclasses.
- 211 2. Use as input data Sentinel-2 with both months. This time, the low resolution will penalize  
212 the frontiers, but there should be an improvement in differentiating agricultural or forest  
213 superclasses.
- 214 3. It does not make sense to use Sentinel-1 or topographical data all alone because most of its  
215 information is about elevation or reflectivity. But combining those, with the orthophoto and  
216 Sentinel-2 the results should improve.

217 To better visualize the results, we have compressed the data in a four superclasses confusion matrix  
218 (Figure 13) and mean intersection over union metrics (Figure 15) as recommended in COCO dataset  
219 [12]. In Appendix D there is confusion matrix and a mean intersection over union for all the 41  
220 classes.

221 As we stated before, Sentinel-2 outperforms the orthophoto in agricultural and forest zones, but it  
222 loses when we need more resolution as in urban areas. Finally, using the complete dataset gives better  
223 results overall. In Figure 14 there is an example of a segmentation using the complete CatLC dataset.

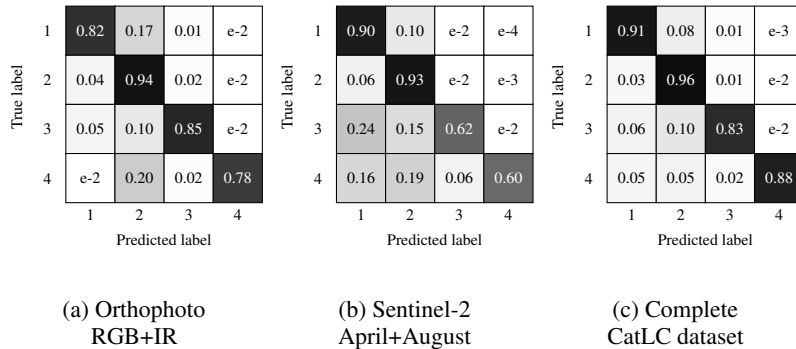


Figure 13: Confusion matrix using different input data. All trained with U-Net neural network. The 41 classes have been compacted to the 4 superclasses (1: agriculture, 2: forest, 3: urban, 4: water).

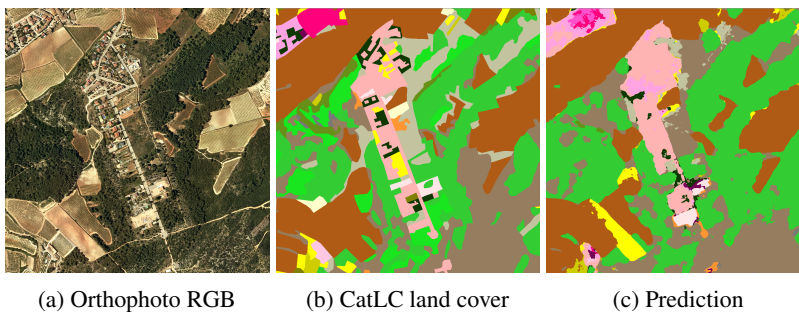


Figure 14: Example of U-Net segmentation.

## 224 5 Discussion

225 The CatLC dataset contains imagery acquired by airborne and satellite sensors at different spectral  
226 bands and spatial resolutions, making it an extraordinary dataset for different AI and DL applications  
227 based on remote sensing data. In the dataset the different types of images are presented with detailed  
228 information on their technical characteristics, and various tutorials are available to facilitate their  
229 use. The volume of data offered is important, approximately 1.4 TB, but the quantity and quality

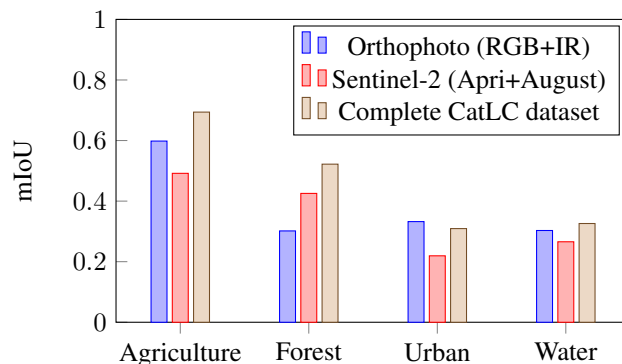


Figure 15: Mean Intersection over Union using different input data for 4 superclasses.

230 of information offered justifies this volume, being a set of remote sensing data open to the public  
 231 with characteristics never seen so far in the AI scientific community. Together with the data, a  
 232 classification study is presented using only a U-Net architecture and orthophoto images (RGB and  
 233 infrared bands). This example can serve as the first step for more complex studies using other  
 234 architectures and the entire set of images provided in CatLC. Studies that can determine for example,  
 235 what type of architectures are more suitable for classifying land covers, and what type of images  
 236 provide more information and which ones can be discarded due to their null or low contribution to  
 237 the final result.

238 CatLC offers images from ICGC’s airborne sensors and ESA Sentinel satellites, which have been  
 239 treated both geometrically and radiometrically for ease of use, even for non-expert users in remote  
 240 sensing applications. Therefore, the purpose of this publication is to open this type of data to the  
 241 expert scientific community in AI so that they can analyze the data, develop new methodologies  
 242 and share their results. The benefits of these investigations will result in automation of production  
 243 processes that are currently carried out almost manually, as is the case of the land cover mapping,  
 244 and in the possibility of updating products almost continuously, only depending on the availability of  
 245 images. This last point should not represent an obstacle in the future, as satellites with remote sensing  
 246 sensors that continuously monitor the Earth are increasingly available. Finally, it should be noted that  
 247 CatLC, although focused on creating the land cover map, is open to all kinds of applications related  
 248 to territory management.

## 249 Acknowledgments

250 This research was funded by industrial doctorate grant 2018-DI-0045 of AGAUR between University  
 251 of Barcelona and Cartographic and Geological Institute of Catalonia and RTI2018-095232-B-C21,  
 252 2017SGR1742 grants. We want also to acknowledge the work of photointerpreters at the Earth  
 253 Observation Area (CSPCOT) at Cartographic and Geological Institute of Catalonia, and thank Anna  
 254 Tardà and Vicenç Palà for their support regarding Sentinel-2 images.

## 255 References

- 256 [1] Carlos García, Jordi Vitrià, and Oscar Mora. Uncertainty-Based Human-in-the-Loop Deep  
 257 Learning for Land Cover Segmentation. *Remote Sensing MDPI*, 2020.
- 258 [2] ImageNet. <https://www.image-net.org/index.php>, 2015.
- 259 [3] PASCAL VOC. <http://host.robots.ox.ac.uk/pascal/VOC/>, 2005.
- 260 [4] Markus Gerke, Franz Rottensteiner, Jan Wegner, and Gunho Sohn. ISPRS semantic labeling  
 261 contest. *International Society for Photogrammetry and Remote Sensing*, 2014.
- 262 [5] Emmanuel Maggiori, Yuliya Tarabalka, Guillaume Charpiat, and Pierre Alliez. Can semantic  
 263 labeling methods generalize to any city? the inria aerial image labeling benchmark. In *IEEE*  
 264 *International Geoscience and Remote Sensing Symposium (IGARSS)*. IEEE, 2017.

- 265 [6] Adam Van Etten, Dave Lindenbaum, and Todd M Bacastow. Spacenet: A remote sensing  
266 dataset and challenge series. *arXiv preprint arXiv:1807.01232*, 2018.
- 267 [7] U.S. Geological Survey. National Land Cover Database, New York. <https://cugir.library.cornell.edu/catalog/cugir-009031>, 2016.
- 269 [8] Seyed Majid Azimi, Corentin Henry, Lars Sommer, Arne Schumann, and Eleonora Vig.  
270 Skyscapes fine-grained semantic understanding of aerial scenes. In *Proceedings of the*  
271 *IEEE/CVF International Conference on Computer Vision (ICCV)*, October 2019.
- 272 [9] Maryam Rahnemounfar, Tashnim Chowdhury, Argho Sarkar, Debvrat Varshney, Masoud Yari,  
273 and Robin Murphy. Floodnet: A high resolution aerial imagery dataset for post flood scene  
274 understanding. *arXiv preprint arXiv:2012.02951*, 2020.
- 275 [10] Centre de Recerca Ecològica i Aplicacions Forestals. Llegenda MCSC-3v2 i MCSC-4 / SIOSE-2  
276 Codificació de les cobertes. [https://www.creaf.uab.es/mcsc/textos/LlegendaMCSC4\\_SIOSE2\\_CATALA.pdf](https://www.creaf.uab.es/mcsc/textos/LlegendaMCSC4_SIOSE2_CATALA.pdf), 2013.
- 278 [11] Olaf Ronneberger, Philipp Fischer, and Thomas Brox. U-net: Convolutional networks for  
279 biomedical image segmentation. In *International Conference on Medical image computing and*  
280 *computer-assisted intervention*, pages 234–241. Springer, 2015.
- 281 [12] Tsung-Yi Lin, Michael Maire, Serge Belongie, James Hays, Pietro Perona, Deva Ramanan, Piotr  
282 Dollár, and C Lawrence Zitnick. Microsoft coco: Common objects in context. In *European*  
283 *conference on computer vision*, pages 740–755. Springer, 2014.
- 284 [13] ESA. Sentinel Application Platform (SNAP). <https://step.esa.int/main/toolboxes/snap>, 2020.
- 286 [14] Magdalena Main-Knorn, Bringfried Pflug, Jerome Louis, Vincent Debaecker, Uwe Müller-  
287 Wilm, and Ferran Gascon. Sen2Cor for Sentinel-2. In *Image and Signal Processing for Remote*  
288 *Sensing XXIII*, volume 10427, page 1042704. International Society for Optics and Photonics,  
289 2017.

290 **Checklist**

- 291 1. For all authors...
- 292 (a) Do the main claims made in the abstract and introduction accurately reflect the paper's  
293 contributions and scope? [Yes]
- 294 (b) Did you describe the limitations of your work? [Yes] See Section 3.
- 295 (c) Did you discuss any potential negative societal impacts of your work? [Yes] The team  
296 has discussed if there are any potential negative societal impacts and agreed that there  
297 are not. The dataset presented is an earth observation dataset (land cover map) that  
298 aims to be a tool for territory management, and as such, to provide a more ethical  
299 and social approach to territory management (in terms of climate change, security,  
300 and preparedness). Indeed, the dataset is a tool to assess natural hazards and territory  
301 changes that are vital to address and evaluate societal impacts of a different kind.  
302 However, address the potential future uses of the dataset and consider if there might  
303 be a breach of the nonmalficence principle by users is out of the scope of this dataset  
304 presentation.
- 305 (d) Have you read the ethics review guidelines and ensured that your paper conforms to  
306 them? [Yes]
- 307 2. If you are including theoretical results...
- 308 (a) Did you state the full set of assumptions of all theoretical results? [N/A]
- 309 (b) Did you include complete proofs of all theoretical results? [N/A]
- 310 3. If you ran experiments (e.g. for benchmarks)...
- 311 (a) Did you include the code, data, and instructions needed to reproduce the main experi-  
312 mental results (either in the supplemental material or as a URL)? [Yes] See Section A.
- 313 (b) Did you specify all the training details (e.g., data splits, hyperparameters, how they  
314 were chosen)? [Yes] See Section 4.
- 315 (c) Did you report error bars (e.g., with respect to the random seed after running ex-  
316 periments multiple times)? [No] The benchmark we present is from doing basic  
317 experiments, mainly to give a starting point to future dataset users.
- 318 (d) Did you include the total amount of compute and the type of resources used (e.g., type  
319 of GPUs, internal cluster, or cloud provider)? [Yes] See Section 4.
- 320 4. If you are using existing assets (e.g., code, data, models) or curating/releasing new assets...
- 321 (a) If your work uses existing assets, did you cite the creators? [Yes] See Section 3.1.
- 322 (b) Did you mention the license of the assets? [Yes] See Section A.
- 323 (c) Did you include any new assets either in the supplemental material or as a URL? [Yes]  
324 See Section A.
- 325 (d) Did you discuss whether and how consent was obtained from people whose data you're  
326 using/curating? [Yes] Data we are using from ESA is open and we indicate that it has  
327 been modified by ICGC.
- 328 (e) Did you discuss whether the data you are using/curating contains personally identifiable  
329 information or offensive content? [Yes] The authors confirm that the dataset does not  
330 contain personally identifiable information or offensive content.
- 331 5. If you used crowdsourcing or conducted research with human subjects...
- 332 (a) Did you include the full text of instructions given to participants and screenshots, if  
333 applicable? [N/A]
- 334 (b) Did you describe any potential participant risks, with links to Institutional Review  
335 Board (IRB) approvals, if applicable? [N/A]
- 336 (c) Did you include the estimated hourly wage paid to participants and the total amount  
337 spent on participant compensation? [N/A]

## 338 **A Appendix**

339 CatLC is available for download, along with all the necessary information and tutorials, on the fol-  
340 lowing website: [https://www.icgc.cat/en/Downloads/Aerial-and-satellite-images/](https://www.icgc.cat/en/Downloads/Aerial-and-satellite-images/Contingut/Catalonia-Multi-resolution-Landcover-Dataset-CatLC)  
341 [Contingut/Catalonia-Multi-resolution-Landcover-Dataset-CatLC](https://www.icgc.cat/en/Downloads/Aerial-and-satellite-images/Contingut/Catalonia-Multi-resolution-Landcover-Dataset-CatLC)

342 There is a tutorial on how to manage the data and visualize it in the following website: <https://github.com/OpenICGC/CatLC/>. There is also the code to reproduce the train presented in the  
343 article. We provide the logs for the hole train that can be visualized using Tensorboard.  
344

345 The use of data is subject to a Creative Common International Recognition 4.0 license. More  
346 information. It contains Sentinel Copernicus data modified by the ICGC. It is also requested that  
347 the methodologies and results obtained by the different scientific groups are shared with the ICGC  
348 through the following e-mail: [catlc@icgc.cat](mailto:catlc@icgc.cat).

## 349 **B Preprocessing**

### 350 **Sentinel-1**

351 The images were processed with the SNAP (Sentinel Application Platform) software [13] from ESA  
352 using the following procedure:

- 353 1. Download of the precise orbit for each image using the “Apply-Orbit-File” function, which  
354 provides detailed information for its correct georeferencing.
- 355 2. Deletion of noisy pixels from the edge of the image using the “Remove-GRD-Border-Noise”  
356 function.
- 357 3. Radiometric calibration of each image providing calibrated reflectivity information for the  
358 Sentinel-1 images. A correct calibration is necessary for the multitemporal study of the data.
- 359 4. Topographic effects Compensation using the “Terrain-Flattening” function. The acquisition  
360 geometry of the SAR images is oblique, which generates distorting artifacts in the reflectivity  
361 associated with the terrain topography (layover, foreshortening and shadowing). This  
362 processing compensates for these artifacts to obtain an image that is as independent as  
363 possible from the topography.
- 364 5. Georeferencing using the “Terrain-Correction” function and final mosaicking of the images.

365 [A video comparing the average Sentinel-1 image and the image for each month is on the CatLC](#)  
366 [webpage.](#)

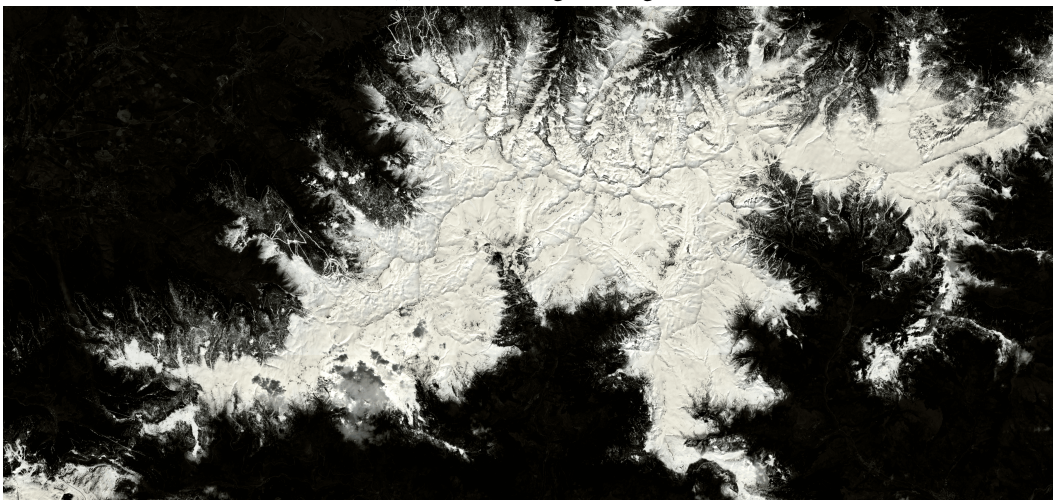
### 367 **Sentinel-2**

368 The images obtained by the MSI sensor from the Sentinel-2A and 2B satellites, from the European  
369 Commission Copernicus program, have been atmospherically corrected by means of the ESA `sen2cor`  
370 `v2.8` software[14] to yield Level-2A images.

371 The main purpose of `sen2cor` is to correct single-date Sentinel-2 Level-1C Top-Of-Atmosphere (TOA)  
372 radiance from the effects of the atmosphere in order to deliver a Level-2A Bottom-Of-Atmosphere  
373 (BOA) reflectance. The process may optionally use a DEM (Digital Elevation Model) to correct  
374 the changes in the radiometry related to the topographic relief. A 10m gridded DEM generated at  
375 ICGC by photogrammetric techniques has been used in this study. A total of 10 bands, at 10m and  
376 20m resolution, are preserved as input features for the Deep Learning process. [Figure 16 presents](#)  
377 [Sentinel-2 images before and after they have been corrected.](#)



(a) Sentinel-2 original image.



(b) Sentinel-2 after corrections.

Figure 16: Sentinel-2 process with atmospheric and topographic corrections.

378 **C Data distribution**

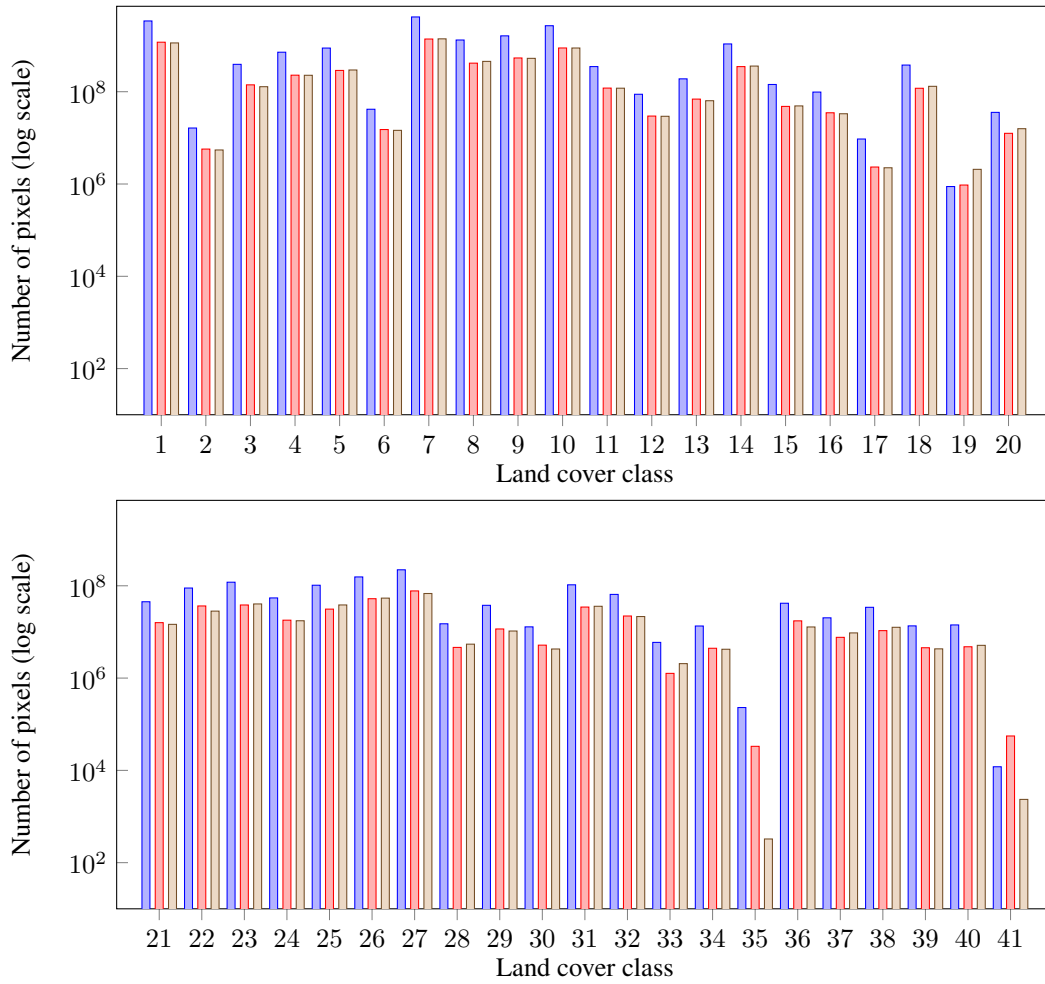


Figure 17: Distribution of the CatLC dataset in three sets: Blue for the train set, red for the validation set and brown for the test set.

379 **D Metrics**

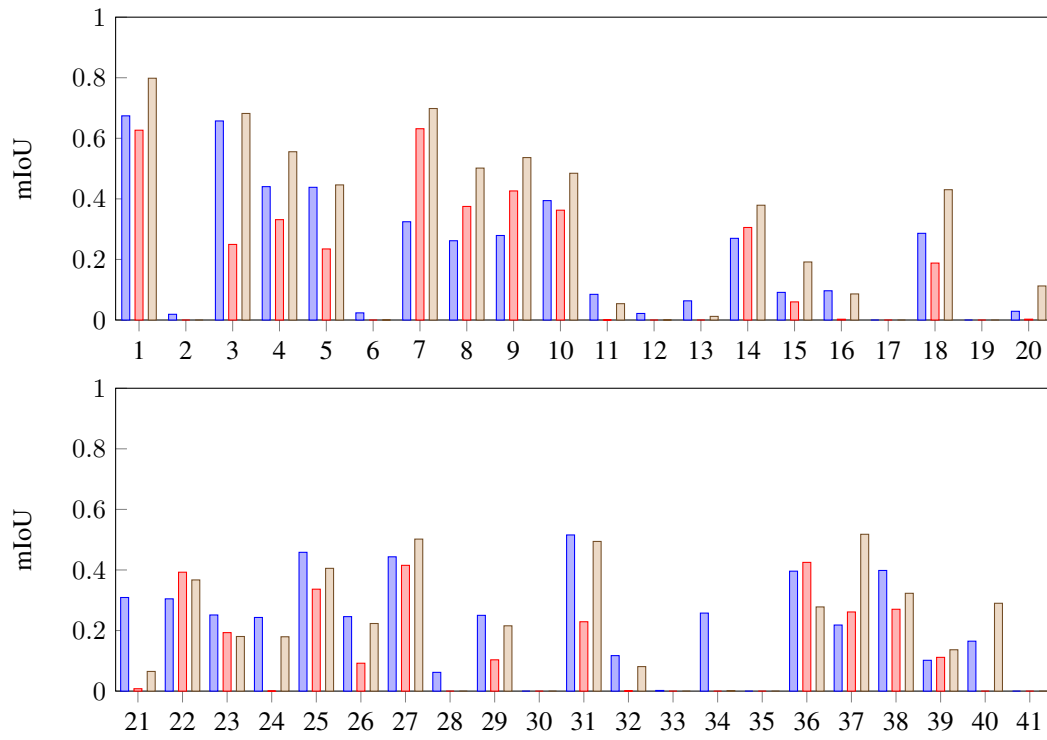


Figure 18: Mean Intersection over Union using different input data for 41 classes.





